Noninvasive Detection of Hypoxic Myocardium Using Fluorine-18-Fluoromisonidazole and Positron Emission Tomography

Gary V. Martin, James H. Caldwell, Michael M. Graham, John R. Grierson, Keith Kroll, Marie J. Cowan, Thomas K. Lewellen, Janet S. Rasey, Joseph J. Casciari and Kenneth A. Krohn

Division of Cardiology, Seattle VA Medical Center, and the Departments of Radiology, Bioengineering, Physiological Nursing and Radiation Oncology, University of Washington, Seattle, Washington

Fluoromisonidazole (FMISO) is metabolically trapped in viable cells as a function of reduced cellular pO_2. Therefore [^{18}F]-FMISO is potentially useful for evaluating patients with hypoxic but viable myocardium. The goal of this study was to investigate [^{18}F]FMISO uptake in ischemic myocardium noninvasively using positron emission tomography (PET). Studies were performed in 10 open-chest dogs subjected to either complete (Group 1, n = 5) or partial (Group 2, n = 5) occlusion of the left anterior descending coronary artery. The tracer was administered by intravenous bolus following the onset of ischemia and serial PET images were acquired for the next 4 hr. In Group 1, viability was assessed using histochemical staining (nitroblue tetrazolium, NBT) and ^{99m}Tc-pyrophosphate (Tc-PYP). In Group 2, viability was assessed using measurements of regional wall motion, histochemical staining and histology (two animals). In each study, PET images obtained at times between 2 and 4 hr postinjection showed specific enhancement of tracer activity in the distal anterior wall and apex of the left ventricle. At 4 hr, the tissue-to-blood pool count ratio was significantly higher in ischemic regions; 1.8 ± 0.4 for Group 1 and 1.6 ± 0.2 for Group 2 versus 1.0 ± 0.1 in nonischemic regions. Postmortem tissue sampling of Group 1 hearts showed significant FMISO retention in samples without evidence for infarction, either by NBT or Tc-PYP deposition, as well as in more severely ischemic regions. In Group 2 animals, FMISO was retained in myocardial regions with reduced blood flow (microspheres), which exhibited improved contraction following reperfusion. We conclude that PET imaging of [^{18}F]FMISO is a promising technique for the noninvasive identification of viable hypoxic myocardium.

J Nucl Med 1992; 33:2202–2208

Fluoromisonidazole (FMISO) and related compounds have been characterized as probes for hypoxic cells in a number of tissues (1–6). Cardiac studies have shown the hypoxia-dependent retention of radiolabeled FMISO in isolated myocytes (5) and in buffer-perfused, isolated hearts (6). In vivo, FMISO accumulates in ischemic myocardium, but not in normally perfused or necrotic myocardium (7,8). More recently, [^{18}F]FMISO has been used to detect myocardial ischemia noninvasively using positron emission tomography (PET), and a potential role for this compound as a marker of tissue viability has been suggested (8). The goal of this study was to further characterize the uptake of [^{18}F]FMISO in ischemic myocardium using positron emission tomography (PET) and to relate its retention in ischemic tissue to regional flow and additional indicators of tissue viability.

METHODS

Animal Preparation and Surgery

Ten mongrel dogs (22–34 kg) were sedated with intravenous thiamyl sodium (20 mg/kg) and intubated. General anesthesia was maintained by mechanically ventilating the animals with Halothane and oxygen. Arterial blood gases were intermittently monitored and ventilatory parameters were adjusted to maintain blood pH between 7.37 and 7.45. Arterial pO_2 in each animal was greater than 200 mmHg. A left thoracotomy was performed, the pericardium opened and a variable hydraulic occluder placed loosely around the left anterior descending (LAD) coronary artery proximal to the first major diagonal branch. Additional catheters were placed in the left atrium, left carotid artery, internal jugular vein and a peripheral foreleg vein. The electrocardiogram and arterial blood pressure were continuously monitored. In five animals, a pair of sonomicrometer crystals were positioned in the myocardium within the LAD distribution to monitor regional systolic wall thickening. For this study, systolic wall thickening was defined as the absolute change in wall thickness occurring between the ECG R-wave and the dichrotic notch of the aortic pressure trace.

Experimental Protocols

Two groups of animals were studied. In Group 1 (n = 5), complete occlusion of the LAD was employed, whereas in Group 2 (n = 5), the LAD was only partially occluded to produce less severe ischemia. Each animal received prophylactic lidocaine (2 mg/kg i.v. bolus followed by a constant infusion of 1 mg/min) to minimize the likelihood of ventricular fibrillation.

Group 1, Complete LAD Occlusion. The purpose of this group of experiments was to study FMISO accumulation under conditions of severe tissue hypoxia, and thus a total occlusion was applied. For Group 1 animals, [18F]FMISO (5–13 mCi) was injected intravenously 15 min following complete LAD occlusion. The reasons for waiting 15 min to inject the FMISO were to allow time for the development of collateral blood flow to the ischemic area and to evaluate the hemodynamic stability of the animal prior to initiation of the PET imaging. In these initial experiments, 3H-FMISO (0.15–0.23 mg/kg, specific activity 13.8 μCi/mg) was injected simultaneously to evaluate whether the two tracers would yield comparable biodistribution data in the heart. Both tracers were synthesized as previously described (9,10). In addition, approximately 1.0 mCi of 99mTc-pyrophosphate (PYP) was injected as a marker of necrosis. Dynamic time of flight PET images were obtained for the next 4 hr. Serial arterial blood samples were obtained throughout the study. Three minutes prior to killing the animal, 201Tl (0.5 mCi) was injected to provide an estimate of relative regional myocardial blood flow (11). Radiolabeled microspheres were not used to measure myocardial blood flow in Group 1 animals to avoid interference in the detection of 3H activity due to Compton scattered electrons from gamma-emitting isotopes in a liquid scintillation counting system. The animals were killed with a lethal intravenous bolus of potassium chloride.

Group 2, Partial LAD Occlusion. Group 2 animals were instrumented with sonomicrometer crystals and a partial stenosis was applied to the LAD with the hydraulic occluder until systolic wall thickening was decreased by approximately 50% (range 30%–65%) from control. During approximately the first 15 min following the stenosis, readjustments of the hydraulic occluder were frequently required to maintain wall thickening in the desired range, presumably secondary to recruitment of collateral blood flow to the ischemic area. After a stable reduction in wall thickening was achieved, [18F]FMISO was injected intravenously and serial PET images were obtained as above. Microsphere myocardial blood flow measurements were made prior to ischemia and at 2 and 4 hr following fluoromisonidazole injection. Radiolabeled (113Sn, 46Sc, 103Ru) 15 micron spheres (3–5·10^6) were injected into the left atrium while a reference organ sample was drawn from the carotid catheter at 15 ml/min for 1 min. Just prior to death the LAD stenosis was removed for 30–60 sec to test for reversibility of the contractile impairment.

Postmortem Tissue Sampling

Postmortem, the heart was rapidly removed, rinsed of excess blood, cut in slices parallel to the image planes and incubated in nitroblue tetrazolium (NBT) to identify areas of infarction. For Group 1 experiments, a single slice corresponding to the middle of one image plane was further sectioned into 16 radial segments which were further cut into 6 transmural pieces for a total of 96 pieces (236 ± 108 mg per piece). Each piece was weighed and counted for 18F, 99mTc and 201Tl activity in a 3-inch NaI well counter, then was solubilized using Instagel (Packard) and H2O2.

Tritium activity was determined by liquid scintillation counting after allowing for decay of the gamma emitting isotopes. Quench correction was done by the external standards method. For Group 2, 16 radial segments were cut into three transmural pieces for a total of 48 pieces (499 ± 162 mg) and counted for 18F and microsphere activity. The gamma well counting and liquid scintillation counting data were corrected for piece weight and normalized as a fraction of the mean normal zone activity

for each heart. The normal zone value was defined as the mean activity of 48 tissue samples taken from the inferior wall of the left ventricle. For Group 1 dogs, each tissue sample was further categorized on the basis of histochemical staining as NBT positive (noninfarcted) or NBT negative (infarcted).

In two Group 2 animals selected at random, 12 of the pieces (6 anterior wall and 6 inferior wall) from each heart were divided and placed in formalin for histologic examination. Two histological stains, hematoxylin and eosin (H&E) and Gomori trichrome (GT) were done on each sample. Pyknosis, loss of nuclear staining, acidophilia of the myocyte and polymorphonuclear leukocyte cellular response were detected by H&E. Banding of the cytoplasm, a characteristic of selective myocardial cell necrosis was detected by GT (12). Initially all slides were reviewed under high power to detect areas of necrosis. Using the GT stained slides, areas of necrosis were traced under low power using a camera lucida (Leitz Dialux 20) and digitized as a percent of the total area of myocardial tissue using computerized planimetry (Hewlitt Packard 9874 A digitizer).

PET

PET was accomplished with the University of Washington time-of-flight system (UWPET). This tomograph was derived from the PETT Electronics SP-3000 PET system and utilizes up to four rings of BaF2 detectors (320 crystals in each ring). The machine acquires emission data in list mode format (writing data to disk, even by event, with timing markers). This format allows selection of time binning and/or gating criteria after the acquisition, preserving maximum flexibility in analysis of data. Images are reconstructed using the reduced-angle confidence-weighted time-of-flight algorithm developed by Snyder (13) and implemented by Politte (14). The reconstructions include corrections for attenuation (based on a measured transmission scan), randoms, and scatter. The system provides a limiting resolution at the center of the field of view of 5 mm in the transaxial plane and either 7.5 or 11 mm in the axial plane (selectable by the operator) (15–17).

For this study, the images were reconstructed with a 12-mm filter, a slice thickness of 11 mm, and a slice separation of 14 mm. Images were integrated over 5 min time intervals during the first hour of each study, and over 30-min intervals for the remainder of each study. Each animal was positioned in the tomograph with a polyurethane mold (custom fitted to each animal) to minimize movement. Final positioning was accomplished by placing a laser beam centered in the first image plane of the machine over the desired position on the exposed heart. Postmortem, the laser beam was used to guide the placement of small needle markers in the image planes to facilitate registration of the image data with the tissue samples. An 18F filled bottle was placed in the image field to permit decay and dead time corrections.

PET Image Analysis

Regions of interest (ROIs) representing 2.0–3.0 cm^3 were defined for the central LV blood pool, distal anterior wall myocardium and inferior wall myocardium, and applied to the serial images to obtain time-activity data. These regions were defined visually by inspection of the attenuation and early [18F]FMISO (blood pool) images and drawn manually using a computer program. A ROI outside the chest was placed for scatter correction. Counts in this ROI were considered "background" and subtracted on a per pixel basis from the entire image. A ROI

encompassing the ^{18}F filled bottle was also placed for the purposes decay and dead time corrections. This correction was performed by multiplying each image by the ratio:

$$\frac{\text{bottle}_{(x)}\text{counts/pixel/min}}{\text{bottle}_{(i)}\text{counts/pixel/min}},$$

where bottle$_{(x)}$ and bottle$_{(i)}$ are the bottle counts in the xth image and in an image obtained just prior to injection of the radiotracer.

Stated statistical comparisons between group means were generally accomplished using the Mann-Whitney U-test. The two-tailed null hypothesis was rejected when the critical value of U was exceeded at a significant level of 0.05. Where p values are given, a two-tailed t-test was used.

RESULTS

PET Images

For each animal, PET images acquired between 2 and 4 hr postinjection showed specific enhancement of activity in the mid to distal anterior wall and apex of the LV (Fig. 1). A representative set of time-activity curves for the LV blood pool and normal and ischemic myocardial regions are shown in Figure 2. Tracer activity in normal myocardium rapidly equilibrates with blood activity and the subsequent clearance curves are virtually superimposable. Activity in ischemic myocardium is low initially but slowly accumulates resulting in a progressive increase in the

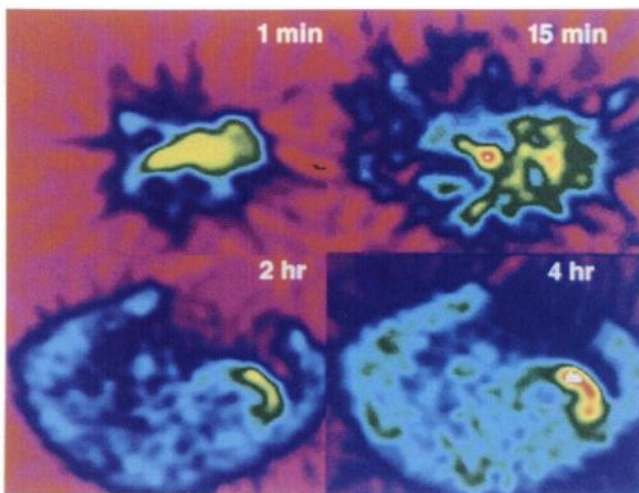### ^{18} F-fluoromisonidazole imaging

FIGURE 1. Serial PET images show [^{18}F]FMISO uptake in ischemic myocardium. The images have not been reoriented and represent a cross section through the chest cavity roughly parallel to the long-axis of the heart. The spine is on the left, while the apex of the left ventricle is to the right. Later images show the outline of the thorax with the thoracotomy opening at the top. At 1 min after injection, the tracer is concentrated in the blood pool, while at 15 min, there is equilibration between blood pool and both normal and ischemic myocardium. The 2-hr image shows slight enhancement of activity in the distal anterior wall and apex of the left ventricule which is more prominent by 4 hr postinjection.
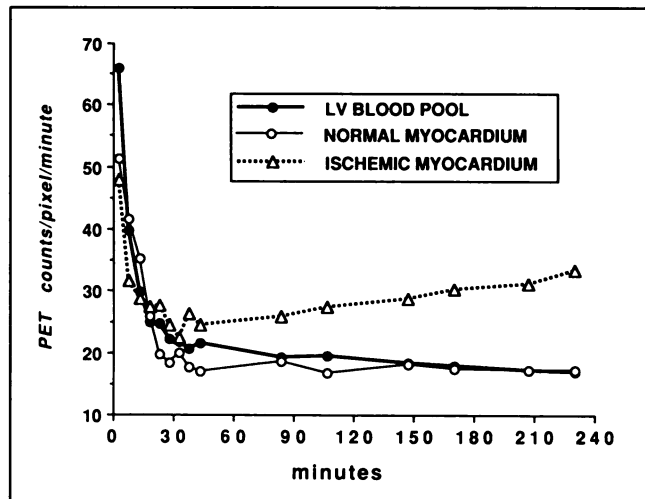

FIGURE 2. Representative time-activity curves for the LV blood pool and normal and ischemic myocardial ROIs. The blood-pool curve is biphasic with a rapid distribution phase and a slower clearance phase. By 5 min postinjection, activity in normal myocardium is equal to that of the blood pool and remains in equilibrium throughout the study. In ischemic myocardium, there is net tracer accumulation between 30 and 240 min.

ischemic ROI-to-normal ROI count ratio. The average myocardium-to-blood pool ratios at various time points out to 4 hr are shown in Figure 3 for both groups of dogs. The ratios were significantly higher for ischemic versus normal myocardium at time points beyond 2 hr.

Tissue Sampling Data

The myocardial tissue samples from Group 1 and Group 2 dogs were analyzed separately. For Group 1 dogs, histochemical staining with NBT showed evidence for non-transmural infarction in each of the five hearts. For the purposes of analysis, we defined the "ischemic" zone as the entire transmural section of the ventricular wall whose lateral edges were demarcated by NBT negative (infarcted) tissue. Typically the ischemic zone contained an admixture of NBT negative samples and more subepicardially located NBT positive samples. The "normal" zone consisted of myocardium entirely outside the ischemic zone. The relationship between the relative regional myocardial blood flow (as estimated by ^{201}Tl deposition) and the relative deposition of ^{99m}Tc-PYP and [^{18}F]FMISO in normal and ischemic myocardium is shown in Figure 4. Relative to the normal zone, flow in NBT positive samples was moderately decreased, 0.59 ± 0.03, $p < 0.05$, and more severely decreased in NBT negative samples, 0.26 ± 0.02, $p < 0.05$. Technetium-99m-PYP values were not significantly elevated in NBT positive samples, 1.17 ± 0.08, but were increased in samples lacking NBT staining, 1.74 ± 0.12, $p < 0.05$. [^{18}F]FMISO deposition was increased to a similar extent in both NBT positive samples 2.98 ± 0.16, $p < 0.05$, and NBT negative samples 2.82 ± 0.13, $p < 0.05$. The tritium and ^{18}F activity in the 96 tissue samples from each of the five hearts were compared by expressing each
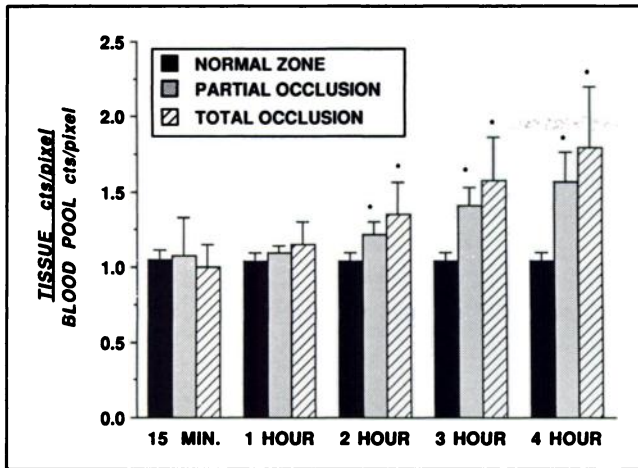
FIGURE 3. Tissue-to-blood pool ratios at various time points following injection of [18F]FMISO. In comparison to normal myocardium, there is a progressive increase in this ratio in ischemic myocardium, both during complete (Group 1) and partial (Group 2) occlusion of the LAD. The data are mean ± s.d. for all 20 normal ROIs and for 10 Group 1 and 10 Group 2 ROIs. * indicates statistically significant differences from normal.

FIGURE 5. The relationship between 3H-FMISO and [18F] FMISO deposition in 96 postmortem tissue samples from a single study is shown and indicates an excellent agreement in the relative deposition of the two tracers.

value as a percent of the injected dose per gram. There was excellent agreement between the two isotopes in each study. Representative data from one study are shown in Figure 5.

To investigate [18F]FMISO binding during less severe ischemia, a partial LAD stenosis was applied during the 4
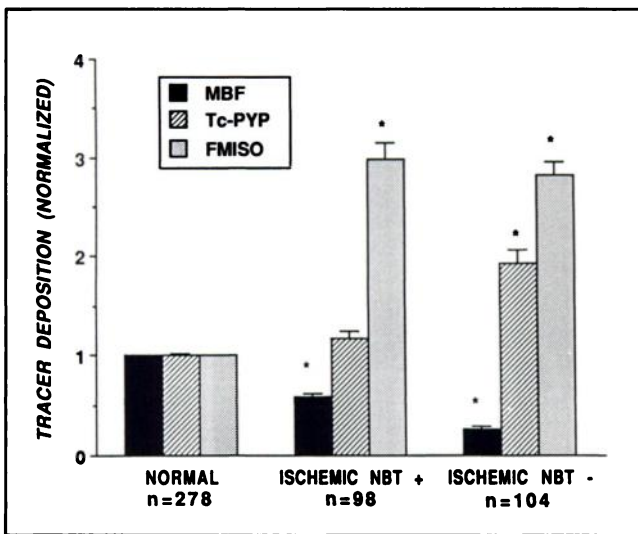
hr imaging period in five animals (Group 2). The wall thickening data are shown in Figure 6. In one animal, wall thickening was reduced by 70% during ischemia and only a slight recovery of function was noted immediately following reperfusion at the end of the study. In this animal, there was NBT evidence for infarction involving the anterior papillary muscle, while no infarction was present by NBT in the four animals showing significant mechanical recovery. Detailed histological examination of two of the Group 2 hearts revealed small areas of selective necrosis in some of the tissue samples taken from the ischemic zone, but the total area of necrosis accounted for no more than 5% of the tissue area in any one of them.

FIGURE 4. Postmortem tissue sampling data from Group 1 dogs showing the relationship between 201Tl (MBF), 99mTc-pyrophosphate (Tc-PYP) deposition and [18F]FMISO (FMISO) deposition in normal myocardium, ischemic-NBT positive (noninfarcted) and ischemic-NBT negative (infarcted) tissue. Whereas both Tc-PYP and FMISO accumulate in samples with histochemical evidence for necrosis, only [18F]FMISO shows enhanced accumulation in tissue samples within the ischemic zone which retained the ability to reduce NBT. NBT = nitroblue tetrazolium. * p ≤ 0.05 versus normal myocardium tissue region.
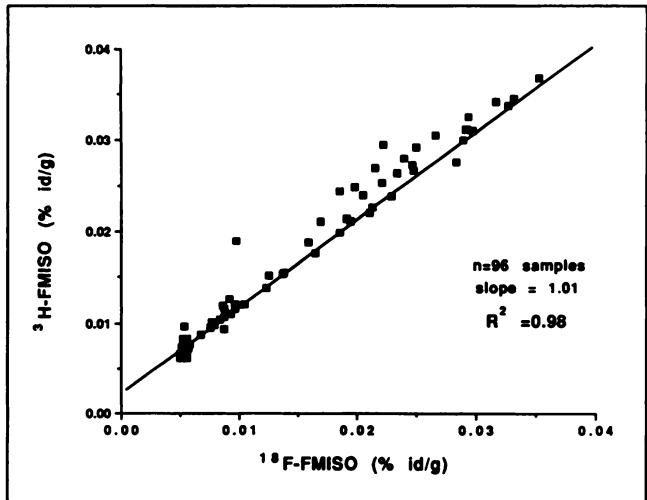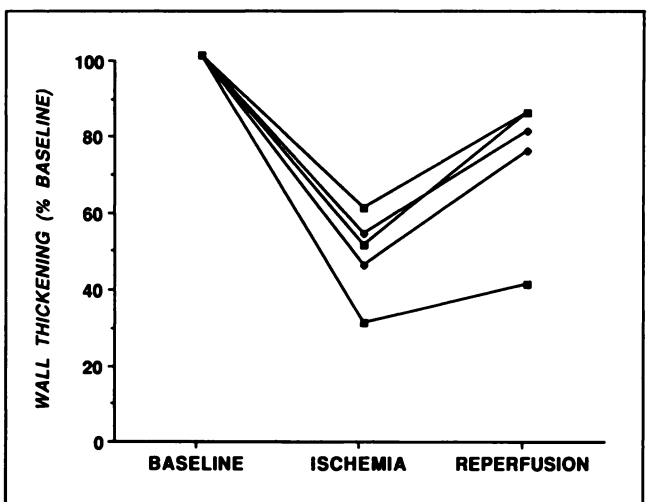

FIGURE 6. Wall thickening data for Group 2 animals. During ischemia, systolic wall thickening was decreased to 30%–60% of normal. Four of the five dogs showed significant improvement following reperfusion.

The microsphere myocardial blood flows and [18F] FMISO data for all Group 2 animals, representing a total of 240 tissue samples are shown in Figure 7. Since in the dogs subjected to partial LAD stenosis the "ischemic" zone could not be identified by NBT staining, tissue samples were categorized as "normal" or ischemic based on their spatial relationship to the epicardial vessels. The myocardial blood flow data are expressed as a ratio of flow during the LAD stenosis (the mean of the two separate microsphere flow measurements made during ischemia) to baseline flow. The fluoromisonidazole data were normalized to the mean value of the normal zone. As shown, there is a fairly uniform deposition of FMISO in normal myocardial samples despite the broad range of flows. In samples taken from potentially ischemic areas in the anterior wall and apex, FMISO deposition and flow were inversely related with maximum normalized FMISO values equal to five.

DISCUSSION

The rationale for evaluating fluoromisonidazole as a probe for myocardial hypoxia is based on in vitro studies showing that this compound and similar molecules are metabolically trapped in cells principally as a function of reduced pO_2 (1-6). While the exact mechanism of trapping in ischemic myocardium is unknown, a general mechanism based on in vitro data and the known biochemistry of nitroimidazoles may be postulated. The drug is lipophilic (octanol:water partition coefficient = 0.42) and diffuses easily from the bloodstream to the tissues. PET time-activity curves suggest that its entry into tissues is delayed,
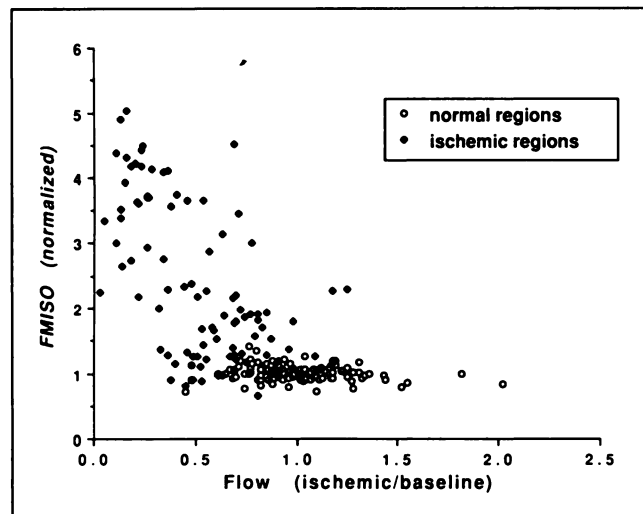

FIGURE 7. Tissue sampling data from all Group 2 animals showing the relationship between [18F]FMISO deposition and microsphere myocardial blood flow in 240 samples. The blood flow data are expressed as the ratio of the flow after the LAD stenosis was applied (the mean of 2 separate microsphere measurements) to the prestenosis (baseline) flow. The [18F]FMISO data in each sample was normalized to the average value in the normal myocardium.

but only slightly, in regions of reduced flow. Figure 3 shows that by 15 min postinjection, FMISO concentrations are on average equal in blood, normal and ischemic tissue.

In cells, FMISO is metabolized by the action of ubiquitous nitroreductase enzymes resulting in the formation of reduced metabolites (18). When oxygen is abundant, the parent FMISO compound is quickly regenerated and metabolites do not accumulate. Thus in normally oxygenated tissue, the distribution of FMISO is a measure of partition coefficient. When cellular pO_2 is low, reduced FMISO metabolites bind to other intracellular molecules which do not as readily leave the cell and thus are "trapped" (19). Isolated cell studies clearly indicate that some metabolites may "back-diffuse" from the cell at a low rate (4,5), but the mechanism and significance of back-diffusion in the intact organ is unknown. Since FMISO trapping is enzyme-dependent, no trapping occurs in metabolically inactive tissue. The strong correlation between 3H- and 18F-labeled FMISO in our study suggests that the image data cannot be explained by the uptake of free 18F in necrotic myocardium.

The results of this study are in general agreement with those of Shelton et al. (8) who first reported the use of [18F]FMISO to image ischemic myocardium with PET. In their study, the myocardial retention of FMISO was higher in dogs in which the tracer was administered within 3 hr of coronary occlusion than in those in which it was given either 6 or 24 hr post occlusion. The authors attributed this result to the greater proportion of jeopardized but viable myocardium which would be expected in dogs with the 3 hr coronary occlusion as opposed to longer occlusions, but direct evidence of tissue viability was not provided.

Our data also support the hypothesis that FMISO can be trapped at levels of hypoxia which do not cause necrosis, and thus may be used as a metabolic probe for ischemic but viable myocardium. By design in the dogs subjected to partial LAD stenosis (Group 2), flow was reduced to a point that contraction was impaired but not abolished. Thus, the myocardium remained functionally viable throughout the study. Furthermore, contractile function improved immediately in four of the five animals when flow was restored (albeit briefly), indicating that the ischemic injury was reversible. As shown in Figure 7, FMISO retention was elevated in some tissue samples which were only mildly underperfused relative to baseline, in which necrosis would not be expected. NBT staining and direct histology (in two hearts) also failed to show significant necrosis in this study.

In Group 1 dogs, coronary occlusion produced more severe ischemia resulting in a transmurally heterogeneous admixture of NBT positive and NBT negative tissue. The finding of FMISO uptake in NBT positive samples with minimally increased PYP and modestly decreased flow (thallium) indirectly supports the notion that FMISO

marks hypoxic but viable tissue. However, FMISO uptake was also enhanced in samples in which necrosis was clearly evident by NBT and PYP, seemingly contradicting the notion that FMISO is trapped in ischemic but viable tissue, but not in dead tissue. It is known that following a total occlusion in dogs, the subendocardial layer of myocardium in the ischemic zone begins to undergo necrosis after 20–30 min and that necrosis proceeds slowly outward towards the subepicardial layer and the full extent of necrosis is not achieved for 3–6 hr (20). Necrosis may reach the epicardium, but more often a rim of epicardial tissue is spared, remaining ischemic but viable. The relative transmural thicknesses of the necrotic and viable tissue are highly variable from dog to dog, depending on the extent of collateral blood flow. Therefore, the avid FMISO uptake in the Group 1 dogs is not unexpected, since the tracer was given only 15 min after the onset of ischemia, at a time when the tissue was intensely hypoxic but had not yet become necrotic. During the subsequent 4 hr, continued uptake and permanent trapping in cells not yet necrotic, but destined to become so, would be expected. This suggests that FMISO may not reliably distinguish viable from nonviable tissue when it is administered during acute severe ischemia, when hypoxic cells rapidly undergo a transition from reversible to irreversible injury. A more promising potential clinical application is the detection of hypoxic myocardium in the convalescent phase of acute myocardial infarction or in patients with chronically ischemic but viable (hibernating) myocardium.

A recognized limitation of this study is that it does not provide direct evidence that FMISO is not taken up when given at a time when the tissue is already necrotic. However, data from other systems has shown that FMISO trapping is enzyme mediated and does not occur in dead cells (4). In the studies by Shelton et al. (8), some of the animals were given FMISO after 24 hr of coronary occlusion and no or minimal FMISO uptake was found.

In the current studies, we imaged for 4 hr following FMISO injection to maximize the information obtained from each study. An image "hot spot" was generally observable after about 2 hr. This delayed appearance of a hot spot reflects the 4.5 hr plasma clearance half-time of this drug (7) and the relatively low absolute rates of FMISO trapping in tissue. Clinical application of this drug might require delayed imaging protocols similar to that used for redistribution thallium imaging. However, examination of the time-activity curves (Fig. 2) shows clear differences in the curves for normal and ischemic myocardium at times prior to 2 hr, suggesting that the development of appropriate tracer kinetic models might allow shorter imaging protocols to be used. Shelton et al. imaged for just 45 min following injection and were able to show differences between experimental groups of animals by dividing the 45 min FMISO image by a $H_2{}^{15}O$ image (8). Further studies are needed to define the optimal imaging protocol for this molecule.

Another potential limitation of this study is the use of the LV blood-pool region of interest as an index of the arterial blood activity in dog hearts due to the potential for "spillover" of tracer activity from the myocardium to the blood pool. Spillover and "partial volume" effects likewise complicate the quantitation of myocardial wall activity. In the current study, no attempt was made to correct either the blood-pool or myocardial wall data for spillover or partial volume effects. While this is a clear limitation of the analysis, it is unlikely that making corrections for spillover or partial volume effects would have substantially changed the conclusions of the study, for the following reasons. There is substantial tissue sampling data from the heart and other organs showing that the tissue-to-blood ratios in nonhypoxic tissue at time points from 30 min–240 min are approximately 1.0, with exceptions being the liver and kidneys where it is higher (7). In the current study, serial blood samples were collected and the tissue-to-blood ratio, using the blood sample collected at 4 hr just prior to death, for the nonischemic myocardial samples from the inferior wall of the LV was 1.02 ± 0.06. This is in good agreement with the "normal zone" tissue-to-blood-pool ratios shown in Figure 3, which are also slightly in excess of 1.0. Thus we do not believe that the blood-pool values taken from the LV cavity are substantially in error. The expected effect of spillover of myocardial wall counts from the ischemic regions to the LV cavity would be to increase LV cavity counts at the late time points. At the same time, partial volume effects would lead to an apparent decrease in counts in the ischemic LV wall due to its proximity to the LV cavity and the lung. The net effect would be to decrease the apparent tissue-to-blood-pool ratio in the ischemic region. Thus, correcting for these effects would lead to even greater estimates of FMISO uptake in ischemic regions. We did not use the left atrial region of interest to estimate blood-pool activity since we were able to acquire images in only two planes in these experiments, and a suitable left atrial cavity signal was not consistently present in all of the studies.

CONCLUSIONS

In conclusion, FMISO is an important and novel addition to the growing list of compounds used to study myocardial blood flow and metabolism with PET. Myocardial pO_2 is determined by a multiplicity of factors including blood flow, blood oxygen content, tissue extraction and utilization. Therefore, any assessment of tissue oxygenation based on a single parameter, for example blood flow, is necessarily incomplete. Because its retention in tissue is linked to cellular pO_2, PET imaging of [^{18}F] FMISO should allow an assessment of whether or not oxygen transport to tissues is matched to metabolic demands and thus may offer advantages as a diagnostic tool. Ultimately, the development of gamma emitting analogues (21) may permit the use of this strategy with single-photon emission computed tomography.

REFERENCES

1. Chapman JD, Baer K, Lee J. Characteristics of the metabolism-induced binding of misonidazole to hypoxic mammalian cells. *Cancer Res* 1983;43:1523–1528.
2. Hoffman JM, Rasey JS, Spence A, Shaw D, Krohn K. Binding of the hypoxia tracer [³H]misonidazole in cerebral ischemia. *Stroke* 1987;18:168–176.
3. Koch CJ, Stobbe CC, Baer KA. Metabolism induced binding of C-14 misonidazole to hypoxic cells: kinetic dependence on oxygen concentration and misonidazole concentration. *Int J Radiat Oncol Biol Phys* 1984;10:1327–1332.
4. Rasey JS, Grunbaum Z, Magee S, Nelson NJ, Olive PI, Durand RE, Krohn KA. Characterization of radiolabeled fluoromisonidazole as a probe for hypoxic cells. *Radiat Res* 1987;111:292–304.
5. Martin GV, Cerqueira MD, Caldwell JH, Rasey JS, Embree I, Krohn KA. Fluoromisonidazole: a metabolic marker of myocyte hypoxia. *Circ Res* 1990;67:240–244.
6. Shelton ME, Dence CS, Hwang DR, Welch MJ, Bergmann SR. Myocardial kinetics of fluorine-18 misonidazole: a marker of hypoxic myocardium. *J Nucl Med* 1989;30:351–358.
7. Martin GV, Rasey JS, Caldwell JC, Grunbaum Z, Krohn KA. Fluoromisonidazole uptake in ischemic canine myocardium. *J Nucl Med* 1989;30:194–201.
8. Shelton ME, Dence CS, Hwang D-R, Herrero P, Welch MJ, Bergmann SR. In vivo delineation of myocardial hypoxia during coronary occlusion using fluorine-18 fluoromisonidazole and positron emission tomography: a potential approach for identification of jeopardized myocardium. *J Am Coll Cardiol* 1990;16:477–485.
9. Grunbaum Z, Freauff SJ, Krohn KA, Wilbur DS, Magee S, Rasey JS. Synthesis and characterization of congeners of misonidazole for imaging hypoxia. *J Nucl Med* 1987;28:68–75.
10. Grierson JR, Link J, Mathis CA, Rasey JS, Krohn KA. A radiosynthesis of [F-18]fluoromisonidazole. *J Nucl Med* 1989;30:343–350.
11. Nielsen AP, Morris KG, Murdock R, Bruno FP, Cobb FR. Linear relationship between the distribution of thallium-201 and blood flow in ischemic and nonischemic myocardium during exercise. *Circulation* 1980;61:797–801.
12. Reichenbach D, Benditt EP. Catecholamines and cardiomyopathy: the pathogenesis and potential importance of myofibrillar degeneration. *Hum Pathol* 1970;1:125–150.
13. Snyder DL, Politte DG. Image reconstruction from list mode data in an emission tomography system having time-of-flight measurements. *IEEE Trans Nucl Sci* 1983;20:1843–1849.
14. Politte DG, Hoffman GR, Beecher DE, Ficke DC, Holmes TJ, Ter-Pogosssian MM. Image reconstruction from Super PETT I: a first-generation time-of-flight positron-emission tomograph. *Trans Nucl Sci* 1986;33:428–434.
15. Lewellen TK, Bice AN, Harrison RL, Pencke MD, Link JM. Performance measurements of the SP-3000/UW time-of-flight emission tomograph. *IEEE Trans Nucl Sci* 1988;35:665–667.
16. Lewellen TK, Harrison RL, Bice AN. An experimental evaluation of the effect of time-of-flight information in image reconstructions for the Scanditronix/PETT Electronics SP-3000 positron-emission tomograph preliminary results. *IEEE Trans Nucl Sci* 1989;36:1095–1099.
17. Lewellen TK, Bice AN, Miyaoka RS, Harrison RL. Performance improvements for the SP-3000 time-of-flight positron-emission tomograph. *J Nucl Med* 1990;31:863.
18. Franko AJ. Misonidazole and other hypoxia markers: metabolism and implications. *J Rad Oncol Biol Phys* 1986;12:1195–1202.
19. Whitmore GF, Varghese AJ. The biological properties of reduced nitroheterocyclics and possible underlying biochemical mechanisms. *Biochem Pharm* 1986;35:97–103.
20. Reimer KA, Jennings RB. The "wave front phenomenon of myocardial ischemic cell death. II. Transmural progression of necrosis within the framework of ischemic bed size (myocardium at risk) and collateral blood flow. *Lab Invest* 1979;40:633–644.
21. Martin GV, Biskupiak JE, Caldwell JH, Grierson JR, Krohn KA. Iodovinylmisonidazole: a metabolic marker for myocardial ischemia. *J Nucl Med* 1990;31:833.